Isolation of a new taste-active brandy tannin A: Structural elucidation, quantitation and sensory assessment

Delphine Winstel, Yoan Capello, Stéphane Quideau, Axel Marchal

Isolation of a new taste-active brandy tannin A: structural elucidation, quantitation and sensory assessment

Delphine Winstel [1], Yoan Capello [2], Stéphane Quideau [2,3] and Axel Marchal [1,*]

[1] Univ. Bordeaux, Unité de recherche Œnologie, EA 4577, USC 1366 INRA, ISVV, 33882 Villenave d'Ornon Cedex, France.

[2] Univ. Bordeaux, ISM (CNRS-UMR 5255), 351 cours de la Libération, 33405 Talence Cedex, France.

[3] Institut Universitaire de France, 1 rue Descartes, 75231 Paris Cedex 05, France.

* Correspondence: axel.marchal@u-bordeaux.fr; Tel.: +33-557-575-867

Highlights

- Original approach to search for taste-active compounds in spirits.
- Identification of a new taste-active compound: brandy tannin A.
- Brandy tannin A is an oxidation product of vescalagin.
- Brandy tannin A is mostly present in cognacs.

ABSTRACT

Enjoying a glass of spirits can be one of the delights of life. While it is well known that their taste improves during barrel aging, the molecular explanations of this phenomenon remain largely unknown. The present work aimed at searching for taste-active compounds formed in spirits during aging. An untargeted metabolomic approach using HRMS was applied on "eau-de-vie" of cognac. A fractionation protocol was then performed on brandies to isolate a targeted compound. By using HRMS and NMR, its structure was elucidated for the first time. This new ellagitannin, called brandy tannin A, considerably increased the sweetness of spirits at 2 mg/L. After development of an LC-HRMS quantitation method, it was assayed in various spirits and was detected mainly in cognacs up to 7 mg/L. These findings demonstrate the sensory contribution of this compound and more generally the relevance of combining metabolomics and separative techniques to purify new taste-active compounds.

Key words: Ellagitannin; sweetness; taste-active compounds; quantitation; oak aging.

1. Introduction

Taste is a sense involved in the chemical detection of compounds likely to develop nutritional or toxic properties. Conventionally, humans can distinguish five basic flavours: salty, sour, bitter, sweet and umami. Many taste-active molecules, belonging to various chemical families, have been identified in numerous plants (Kinghorn, 1987). The investigation of these products in natural matrices such as foods or beverages is a major challenge for chemists. Such studies are particularly relevant in oenology since they allow a better understanding of the taste of wines and spirits.

In recent years, oenological research has enabled the molecular characterization of non-volatile compounds involved in the perception of taste, as well as tactile sensations. To isolate such sensory-active molecules, several strategies have been developed. First, inductive fractionations guided by sensory analysis were implemented by using various separation techniques (Frank et al., 2006; Marchal, Waffo-Téguo, et al., 2011). Another strategy was to search for structural analogues to already known taste-active compounds on the basis of their putative empirical formulas (Gammacurta et al., 2019; Marchal, Génin, et al., 2015). Then, analogues were isolated following targeted purification with liquid chromatography-high resolution mass spectrometry (LC-HRMS) screening and were tasted to determine their sensory properties. More recently, a new method that combines untargeted and targeted approaches in the search for new natural products was proposed and applied to spirits (Winstel et al., 2021). However, the molecular determinants associated with sweet or bitter taste have only been partially elucidated. These perceptions are linked in particular to the presence of several compounds released during winemaking by grapes (Cretin et al., 2019; Fayad et al., 2021), yeasts (Marchal, Marullo, et al., 2011) or by oak wood (Gammacurta et al., 2019; Marchal, Cretin, et al., 2015; Saucier et al., 2006).

Used for a long time as shipping devices, oak barrels are now mainly used for producing wines and spirits, owing to the physico-chemical and sensory changes they cause. The non-volatile compounds associated with modifications of colour (Chassaing et al., 2010), tactile sensations (Glabasnia & Hofmann, 2006) and taste (Marchal, Waffo-Téguo, et al., 2011) that are consecutive to the aging of wines and spirits have been studied in recent decades. Empirically, the observations of winemakers suggest an increase in sweetness of wines and spirits during oak wood aging. This observation has been confirmed (Marchal et al., 2013), interpreted at the molecular level, and was found to be due to the release of glucosylated and galloylated triterpenoids called quercotriterpenosides (QTT) (Gammacurta et al., 2019; Marchal, Waffo-Téguo, et al., 2011). On the contrary, excessive or inappropriate use of oak wood can increase bitterness in wines and spirits. This phenomenon is mostly attributed to polyphenols such as lignans (Marchal, Cretin, et al., 2015) and coumarins (Winstel et al., 2020). Moreover, the ellagitannins of oak wood have been extensively studied for their possible health effects (Auzanneau et al., 2012; Cardullo et al., 2020; Georgess et al., 2018), as well as for their sensory properties (Chira et al., 2015).

Even if the bitter characteristics of the main ellagitannins have been suggested and their gustatory detection threshold established (Glabasnia & Hofmann, 2006), the concentrations observed in wines are significantly below these thresholds. In spirits, the main hydrolysable tannins, such as vescalagin, castalagin, roburins A to E and grandinin, have been identified (Gadrat et al., 2020; Puech et al., 1990). However, they seemed to be extracted from oak wood into “eau-de-vie” from the beginning of barrel aging and were quickly degraded (Viriot et al., 1993). Likewise and by comparison with the concentrations obtained in various spirits, no clear correlation could be established between these compounds and the bitterness sometimes perceived in oaked brandies (Gadrat et al., 2020; Glabasnia & Hofmann, 2006). Since spirits are a highly complex matrix characterized by an ethanol concentration that is

usually between 36% to 55% (*v/v*), ellagitannins may be involved in various chemical reactions, including hydrolysis, solvolysis and oxidation. For instance, Quideau *et al*. reported that in an ethanol solution of vescalagin, the C-1 epimer of castalagin was converted to *β*-1-*O*-ethylvescalagin (Quideau et al., 2005). This ethanol adduct has been identified in wines (Saucier et al., 2006), but never in spirits. Moreover, Fujieda *et al.* discovered oxidation products of castalagin, named whiskey tannins A and B, in Japanese whiskey (Fujieda et al., 2008). Their structure suggested that they were formed by regioselective oxidation of the pyrogallol ring linked at the glucose C-1 position of castalagin, and subsequent addition of ethanol followed by a benzilic acid-type rearrangement. Therefore, spirits aging can lead to the formation of new chemical species from oak extractables. A recent study provided confirmation by showing that the diversity of compounds in aged spirits is greater than in the wood itself (Roullier-Gall et al., 2018). This finding suggests that non-volatiles of oaked spirits are both native compounds released from wood and molecules newly formed during aging. Further knowledge is needed to better understand how such changes in the chemical composition of spirits are linked the overall improvement of their sensory quality during aging.

To search for new taste-active compounds in spirits, the recently proposed combination of untargeted and targeted approaches was implemented in the present work. First, untargeted metabolomic profiling by HRMS was carried out on several “eau-de-vie” of cognac of different vintages. Statistical analyses were performed to evaluate the overall structure of the metabolomic data and to select compounds potentially newly formed in spirits. Then, a targeted fractionation protocol, including liquid-liquid extractions, centrifugal partition chromatography (CPC) and preparative-HPLC, allowed the isolation of new taste-active compounds that can be further identified, characterized for their sensory properties, and quantitated in spirits.

2. Materials and methods

2.1. Chemicals

HPLC grade solvents (acetonitrile, ethanol (EtOH), ethyl acetate (EtOAc), *n*-heptane, propan-2-ol, methanol and butan-1-ol (BuOH) from VWR International, Pessac, France and methyl *tert*-butyl ether (MTBE) from Acros Organics, Fisher Scientific, Illkirch, France) and ultrapure water (Milli-Q purification system, Millipore, France) were used. LC–HRMS chromatographic separations were performed with deionized ultrapure water, LC–MS grade acetonitrile and formic acid (Optima, Fisher Chemical, Illkirch).

2.2. Samples

A commercial spirit (Cognac XO) and an oak wood extract (100 g/L), prepared in a hydro-alcoholic solution (50:50 H_2O/EtOH) for three days, were screened by LC-HRMS.

For targeted compound isolation, a blend of "eau-de-vie" (EDV) of cognac aged in barrels for 19, 20 and 21 years, was used.

For quantitative analysis, 36 commercial spirits aged in oak wood were assayed. The second set of spirits consisted of 9 vintages of EDV of cognac. The samples were not commercial cognac but EDV still in barrels. They corresponded to a real aging kinetics, i.e. samples of the same EDV were collected each year in the same barrel. The third set of spirits (Table S1, Supplementary data) consisted of ten different vintages of EDV of cognac, still in barrels. The samples came from the same distillery, had undergone similar aging conditions, and had been matured in used barrels (350 L coarse-grained oak barrels). A sample was collected from five different barrels for each year (except for 1970 and 1973 for which only four replicates were available).

All spirits were provided by the House of Rémy-Martin. They were diluted with water by a factor 5 and then filtered at 0.2 µm. This dilution factor was considered when calculating the final concentration.

2.3. LC-Analysis

For the screening and quantitative analysis, the UHPLC appliance consisted of a Vanquish system (Thermo Fisher Scientific, Les Ulis, France) with binary pumps, an autosampler and a heated column compartment. For LC-HRMS analyses and quantitation, a Hypersil Gold C_{18} column (100 × 2.1 mm, 1.9 µm, Thermo Fisher Scientific) was used as the stationary phase, with water (Eluent A) and acetonitrile (Eluent B), containing both 0.1% of formic acid, as mobile phases. The flow rate was set at 600 µL/min and the injection volume was 2 µL. The temperature of the column chamber was set at 30°C in forced air mode. For screening analysis, eluent B varied as follows: 0 min, 10%; 1.0 min, 10%; 5.0 min, 50%; 5.3 min, 98%; 6.0 min, 98%; 6.15 min, 10%; 7 min, 10%. For the quantitative analysis, eluent B varied as follows: 0 min, 10%; 1.6 min, 10%; 5.3 min, 35%; 6.1 min, 98%; 7.1 min, 98%; 7.3 min, 10%; 8.3 min, 10%.

2.4. HRMS

For the screening and quantitative analysis, an Exactive Orbitrap mass spectrometer was equipped with a heated electrospray ionization (HESI-II) probe (both from Thermo Fisher Scientific). The ionization and spectrometric parameters were designed for each type of analysis and are summarized in Table 1. Optimization of gas values, voltages and temperatures applied for ionization and ion transfer was carried out in negative mode.

Detection of the targeted compound was based on the theoretical exact mass of its deprotonated molecular ion ($[M - H]^-$) and its retention time. Peak areas were determined by automatic integration of extracted ion chromatograms (XIC) built in a 3-ppm window around its exact mass. All data were processed using the Qual Browser and Quan Browser applications of Xcalibur version 3.0.

2.5. Metabolomic approach

Untargeted metabolomic profiling by HRMS on several EDV of Cognac of different vintages has already been described in a previous study (Winstel et al., 2021). The analysed samples corresponded to the third test of spirits (Table S1, Supplementary data). For this approach, a Q-Exactive Plus mass spectrometer with a HESI-II probe (Thermo Fisher Scientific) was used and the HPLC appliance consisted of a Waters Acquity I-Class UPLC system (Waters, Guyancourt, France). Optimization of gas values, voltages and temperatures applied for ionization and ion transfer was carried out in negative mode (Table 1). After analysing the spirits samples, Thermo RAW files were exported to the open-source software package MZmine 2 (2.38 version) for data processing (Pluskal et al., 2010). All the statistical analyses were carried out using the open-source software R Statistical (Foundation for Statistical Computing, Vienna, Austria). Results were interpreted by one-way analysis of variance (ANOVA), using *vintage* as factor. Principal Component Analysis (PCA) was performed on normally distributed data. K-means clustering was also established for data classification (package ClassDiscovery). Pearson correlations were then carried out ($\alpha<0.05$, correlation coefficient $r>0.8$) and allowed the creation of groups of compounds with a similar evolution according to the vintages.

2.6. Extraction and isolation

2.6.1. Liquid-liquid extractions

The blend of EDVs used for isolation was titrated around 64% vol. alc. It was evaporated to dryness *in vacuo* to remove the ethanol. After evaporation and freeze-drying of four bottles of 750 mL of EDV, a dry extract of 7.35 g was obtained. To start the liquid-liquid extractions, the extract was first solubilized in 900 mL of milli-Q water. This aqueous extract was washed twice with 450 mL of *n*-heptane. This aqueous layer was then extracted successively with MTBE (6×500 mL), EtOAc (5×800 mL) and with water-saturated BuOH (4×800 mL). The combined organic layers were evaporated *in vacuo*, suspended in water, and freeze-dried

184 twice to obtain brownish powders of MTBE (1.8 g), EtOAc (1.3 g), BuOH (1.2 g) and
185 aqueous (3 g) pre-purified extracts. They were stored under air- and light-protective
186 conditions.

187 *2.6.2. CPC fractionation*

188 CPC was performed on a Spot prep II LC coupled with a SCPC-100+1000 (Armen
189 Instrument, Saint-Avé, France), both controlled by Armen Glider Prep V5.0 software. A 1 L
190 rotor was used. The solvent was pumped into the column by a 4-way quaternary high-pressure
191 gradient pump. The samples were introduced into the CPC column *via* an automatic high-
192 pressure injection valve. All the experiments were conducted at room temperature with UV
193 detection at 254 and 280 nm. Following the procedure described by Marchal *et al*. (Marchal,
194 Waffo-Téguo, et al., 2011), the selection of an appropriate biphasic system of solvents was
195 based on the study of the partition of extract compounds in both phases. Several systems were
196 tested, and the BuOH extract was fractionated using the ternary biphasic system
197 EtOAc/propan-2-ol/H_2O (3:1:3, v/v/v). Separation was carried out by one CPC run of 1.2 g
198 injection. Experiment was performed at 1200 rpm in ascending mode with a flow rate of 30
199 mL/min for 135 min for the elution phase and 50 mL/min for 40 min for the extrusion. The
200 Spot Prep fraction collector was set to 25 mL/min. Every 10 CPC tubes, 200 µL were taken,
201 evaporated, dissolved in 1 mL of H_2O/MeOH 90:10 (v/v), filtered and analysed by LC-
202 HRMS. Ten fractions, named F-I to F-X, were formed according to their similar
203 chromatographic profile, after being combined, evaporated *in vacuo*, suspended in water, and
204 freeze-dried.

205 *2.6.3. Preparative liquid chromatography*

206 Preparative HPLC analyses were performed using a Waters Prep 150 LC including a 2545
207 Quaternary Gradient Module, a 2489 UV/Visible detector (Waters). Final purification of
208 targeted compound 1 (TC1), which was present in the CPC fractions F-II (83.2 mg), F-III

(144.9 mg) and F-IV (62.8 mg), was achieved by preparative HPLC using columns chosen after LC-HRMS tests. Separations were carried out using a Hypersil Gold C18 (20 mm × 250 mm, 5 µm, Thermo Fisher Scientific) equipped with a Hypersil Gold preparative C18 guard cartridge (20 × 10 mm, 5 µm, Thermo Fisher Scientific). The mobile phase was a mixture of ultrapure water (Eluent A) and acetonitrile (Eluent B), both containing 0.1% of formic acid. The flow rate was set to 20 mL/min. Eluent B varied as follows: 0 min, 10%; 7.4 min, 10%; 44.2 min, 30%; 46.4 min, 98%; 59 min, 98%; 60 min, 10%; 66 min, 10%. Aliquots (20 mg) of CPC fractions were dissolved in 400 µL of H_2O/MeOH 60:40 (v/v), 0.2 µm-filtered and introduced manually into the system. UV detection was performed at 280 nm and chromatographic peaks were collected manually just after the detector. The pure compound solution was evaporated *in vacuo* to remove acetonitrile and freeze-dried to obtain a pale-yellow amorphous powder (10.2 mg).

Brandy tannin A (TC1): pale-yellow amorphous powder; $[\alpha]_D^{25} - 77.8$ (c = 0.1, MeOH); HRMS *m/z* 703.1143 $[M - H]^-$ ($C_{31}H_{27}O_{19}^-$, 0.6 ppm); ^{1}H NMR [acetone-D_6/D_2O (9:1, v/v), 400 MHz] δ 1.09 (t, J = 7.0 Hz, 3H), 1.16 (t, J = 7.1 Hz, 3H), 3.47 (dq, J = 9.3, 7.0 Hz, 1H), 3.59 (dq, J = 9.4, 7.0 Hz, 1H), 3.77 (m, 1H), 3.86 (m, 1H), 4.18 (m, 2H), 4.28 (d, J = 1.1 Hz, 1H), 4.40 (dd, J = 9.3, 6.7 Hz, 1H), 4.90 (ddd, J = 9.3, 4.3, 2.8 Hz, 1H), 5.32 (d, J = 6.7 Hz, 1H), 5.40 (s, 1H), 5.48 (d, J = 1.0 Hz, 1H), 6.69 (s, 1H); ^{13}C NMR [acetone-D_6/D_2O (9:1, v/v), 100 MHz] δ 201.9, 170.1, 168.6, 168.0, 163.1, 157.9, 146.0, 145.5, 144.5 (2C), 142.6, 136.6, 135.4, 125.4, 125.0, 114.7, 113.5, 111.0, 108.1, 84.6, 80.3, 74.8, 72.7, 67.8 (2C), 65.2, 63.3, 61.9, 45.5, 15.3, 14.0 (Table 2 and Figure S6, supplementary data).

2.6.4. NMR experiments

NMR experiments were conducted on Bruker Avance II 400 and Avance III 600 NMR spectrometers equipped with a 5 mm PA BBO and a 5 mm PA BBI probe, respectively. All 1D (proton, carbon, and DEPT-135) and 2D (COSY, HSQC, HMBC, and ROESY) spectra

were acquired at 298.15 K in a 9:1 (v/v) acetone-D_6/D_2O solvent mixture and were calibrated using residual undeuterated acetone as an internal reference (^1H δ 2.05 ppm; 13C δ 29.8 ppm). Proton, carbon, DEPT-135, COSY and HSQC spectra were obtained on the Bruker 400 MHz spectrometer, and HMBC and ROESY spectra were obtained on the Bruker 600 MHz spectrometer. The following abbreviations were used to describe the multiplicities: s = singlet, d = doublet, t = triplet, q = quartet, m = multiplet. Data analysis was performed with Mnova NMR version 14.2.0.

2.7.Method validation for quantitation

A stock solution of brandy tannin A (1 g/L) was prepared in methanol. One range of calibration was prepared by successive dilutions of this solution in a non-oaked EDV adjusted to 12% v/v with 0.1% of formic acid, in order to supply calibration samples (1 µg/L, 2 µg/L, 5 µg/L, 10 µg/L, 20 µg/L, 50 µg/L, 100 µg/L, 200 µg/L, 500 µg/L, 1 mg/L, 2 mg/L, 5 mg/L and 10 mg/L).

The validation method for quantitating brandy tannin A in spirits was performed by studying linearity, sensitivity, specificity, intraday repeatability, and trueness. The LC-HRMS method sensitivity was established using the approach described by De Paepe *et al*. (De Paepe et al., 2013). Limit of detection (LOD) of a molecule is defined as the lowest concentration at which a reliable and reproducible signal is observed. The signal must be different from a blank performed under the same conditions. The lowest levels of the calibration curve (from 1 to 20 µg/L) were injected into five replicates. Limit of quantitation (LOQ) is defined as the lowest concentration of the molecule that can be quantitatively determined by the method, with a precision lower than 10% and an accuracy (recovery of back-calculated concentrations) higher than 90%. The working range was based on the LOQ previously determined. A calibration curve was determined by plotting the areas for each concentration level versus the nominal concentration. Quadratic regression was used with a 1/x statistical weight. Linearity

was evaluated by correlation coefficient (R^2) and by deviations of each back-calculated standard concentration from the nominal value. To determine intraday precision, five replicates of three intermediate calibration solutions (10 µg/L, 200 µg/L and 10 mg/L) were injected, and the relative standard deviation (RSD%) was calculated. Trueness was checked by calculating the recovery ratio (between measured and expected areas) from two samples of EDV (EDV-1; EDV-2). They were chosen among the analysed samples and were spiked with calibration solution corresponding to an addition of 20 µg/L, 200 µg/L and 10 mg/L of brandy tannin A. Interday repeatability was estimated by injections of the same two samples (10 µg/L and 10 mg/L) for five successive days. Specificity was assessed by evaluating the mass accuracy and retention time repeatability. These parameters were determined concomitantly with the precision and trueness analysis described above.

2.8. Sensory analysis

Taste evaluation was performed in a dedicated room, at room temperature (around 20 °C) (ISO 8589:2010, 2010) and with INAO normalized glass (ISO 3591:1977, 1977). Pure compounds were tasted by five experts (four women, one man, aged from 24 to 54 years old) in wine and spirits tasting, at 2 mg/L in demineralized water (eau de source de Montagne, Laqueuille, France), as well as in a non-oaked EDV adjusted to 40% (v/v). Experts described the gustatory perception (bitterness, sweetness, perception of burning and taste of fat) of the targeted compound using the vocabulary of spirits tasting and were asked to evaluate the intensity on a scale from 0 (not detectable) to 5 (strongly detectable). The panelists were informed of the risks and nature of this study and were asked to give their consent to participate in the sensory analyses. Even though the compound was purified from EDV of cognac, the experts were advised to spit out the samples after tasting.

3. Results and discussion

3.1. Untargeted metabolomic analysis of spirits to select relevant compounds

An untargeted analysis by HRMS was achieved on a series of EDV of cognac of 10 different vintages from 2015 to 1970 (Table S1, supplementary data), as described in a previous study (Winstel et al., 2021). After the U-HPLC-HRMS analysis, the data were processed with the use of MZmine 2 software. Thanks to these treatments, a peaklist of 42,120 negative ions was obtained between *m/z* 100 to 1500, then filtered into a peaklist of 331 ions having an associated data-dependent MS^2 spectrum. PCA of the data was carried out using the peak areas of the 331 negative ions highlighted by the ANOVA. The vintage effect was clearly significant on the first axis and the ANOVA showed that it was significant (p-value <0.05) for 321 compounds out of 331 (97%). The compounds were then divided into different groups showing a similar trend to evolve according to the vintages, by using k-means clustering followed by Pearson correlations. Of the 321 compounds detected in negative mode and significantly influenced by the vintage, 298 were assigned to a group among the four created (Figure S2, supplementary data). Groups 1, 3 and 4 represented 92% of the compounds, whose concentrations were significantly influenced by the vintage and were generally more abundant in older vintages. Group 2 was composed of 24 compounds whose contents increased during 20 years of aging and then slowly decreased.

As in the previous study, the statistical groups (Figure S2, supplementary data) revealed the presence of a wide diversity of molecules in these spirits. For most of them (274/298), the contents were higher in aged spirits, while the opposite was observed for less than 8%. Such a result could be explained by two phenomena: a continuous release of oak native compounds during aging and/or the neoformation of molecules through chemical reactions involving oak extractables. The aim of this study was to focus on compounds that were formed during spirits aging, since they cannot be isolated by focusing on oak wood. Therefore, the peaklist obtained by the MZmine analysis and the data from the statistical analysis were used to target new

309 natural products and attempt to purify them. The compounds of interest were selected
310 according to three criteria: a significant abundance of the targeted compound, a strong
311 increase in concentrations in old vintages, and a large gap in intensity between the
312 concentration in spirits and in oak wood extracts, which could suggest a neoformation rather
313 than an extraction.

314 First, the 298 compounds were classified in a table according to their intensity in the EDV of
315 cognac from 1979 to 2015 (data not shown). Then, they were screened by HRMS in the
316 analysed spirits and in oak wood extracts. Among all the chromatographic peaks, a compound
317 combining the previously defined criteria was observed and targeted for the rest of the study:
318 TC1 with a nominal mass of 703. Its concentration increased until 1995 and then slightly
319 decreased until 1970, while remaining abundant in the EDV of cognac. It was one of the 24
320 compounds present in group 2. XICs were built by targeting the negative ion at *m/z* 703.1143
321 in a 3-ppm window around its theoretical *m/z*. LC-HRMS screening revealed the presence of
322 TC1 only in spirits, which could be explained by a possible chemical reaction in the matrix
323 during aging (Figure S3, supplementary data). Consequently, its purification protocol was
324 carried out using the EDV of cognac.

325 *3.2. Isolation and Identification of TC1 in Spirits*

326 *3.2.1. Purification of TC1 from "eau-de-vie" of cognac*

327 Metabolomic profiling revealed that TC1 was present at higher levels in the EDV aged in
328 barrels for 20 years (Figure S4, supplementary data). Its purification was then carried out
329 from a blend of three EDVs aged in barrels for 19, 20 and 21 years, respectively. First, they
330 were evaporated to dryness to remove ethanol, which could interfere with subsequent
331 fractionation steps. After freeze-drying, the second step consisted of sequential liquid/liquid
332 extractions using MTBE, EtOAc and BuOH to obtain pre-purified extracts. TC1 was mainly
333 present in the BuOH extract, so this fraction was selected to continue the fractionation. The

resulting extract had a complex chromatographic profile with various peaks and co-elutions. The use of the CPC was necessary to fractionate it and obtain a fraction enriched in compound *m/z* 703. Preliminary tests showed that the ternary solvent system EtOAc/propan-2-ol/H_2O (3:1:3, v/v/v) in ascending mode allowed the best partition of the sample. Since many tubes were collected, fractions were constituted by grouping tubes together on the basis of their LC-HRMS profiles. After solvent evaporation and freeze-drying, 10 fractions (noted F-I to F-X) were obtained as powder in variable quantities. Fractions F-II, F-III and F-IV were richer in TC1, so they were submitted to preparative HPLC with UV detection. A first injection of 5 mg of each fraction revealed that the chromatograms exhibited a refined profile with only a few peaks detected both in UV a 280 nm. Therefore, a suitable gradient was chosen for each fraction and F-II, F-III and F-IV were fractionated by successive injections. The peak corresponding to TC1 was collected manually just after UV detection for each fraction to give 10.2 mg of a pale-yellow amorphous powder after acetonitrile removal and freeze-drying.

3.2.2. Structural elucidation of TC1

The resolution, mass accuracy and stability offered by HRMS are particularly useful for the determination of empirical formulas of unknown natural compounds. The HRMS spectrum of TC1 exhibited a quasi-molecular $[M - H]^-$ ion at *m/z* 703.1143. Given the isotopic ratio (around 35% abundance) and the experimental mass (with a delta of 0.6 ppm) of the deprotonated ion, the empirical formula $C_{31}H_{28}O_{19}$ was assigned to TC1. To our knowledge, no compound with this empirical formula has been described in the literature. To investigate the nature and the sequence of the functional groups, fragmentation was performed on the pure molecule by non-resonant activation in the higher collision dissociation (HCD) mode with collision energy of 35 arbitrary units. The fragmentation of TC1 led to the formation of many ions (Figure S5, supplementary data). The *m/z* 657.0731 ion, with the molecular

formula of $C_{29}H_{21}O_{18}^-$, corresponded to a species formed by the loss of a neutral group C_2H_6O regarding the *m/z* 703.1143 ion. This group could correspond to a loss of ethanol. Likewise, the negative *m/z* 639.0626 ion of the empirical formula $C_{29}H_{19}O_{17}^-$ corresponded to a dehydration regarding the *m/z* 657.0731 ion. Furthermore, the fragmentation spectrum showed the presence of a negative ion at *m/z* 523.0513 and could correspond to a species formed by the loss of a $C_6H_{12}O_6$ group from the *m/z* 703.1143 ion, which is characteristic of a hexose. In addition, an ion at *m/z* 169.0134 ($C_7H_5O_5^-$) was observed, which may correspond to a gallic acid. The spectrum also exhibited an ion at *m/z* 300.9991 ($C_{14}H_5O_8^-$). This might reveal the presence of the ellagic acid bislactone in the molecule or a structural unit from which this bislactone could be derived. In addition, ions at *m/z* 249.0404 ($C_{12}H_9O_6^-$) and *m/z* 275.0195 ($C_{13}H_7O_7^-$) were detected. They may be 2,2′,3,3′,4,4′-hexahydroxybiphenyl and 3,4,8,9,10-pentahydroxydibenzo[b,d]pyran-6-one, respectively. These latter three ions at *m/z* 301, 275 and 249 are generally characteristic fragments of the main *C*-glucosidic ellagitannins, such as vescalagin and castalagin (Bowers et al., 2018). Therefore, by comparing the fragments obtained with the data in the literature, TC1 could be a *C*-glucosidic ellagitannin (Engström et al., 2015; Jourdes et al., 2011).

A full characterization by NMR was then carried out to identify the structure of TC1, which was dissolved (5 mg) in a 9:1 (v/v) acetone-D_6/D_2O solvent mixture (Figure S6, supplementary data). The ^1H NMR spectrum displayed only one aromatic signal resonating at 6.69 ppm, several signals in the downfield sector of the aliphatic chemical shift range between about 3.5 and 5.5 ppm, which could be due to resonances of protons attached to sugar-type oxygenated carbon atoms, and two diagnostic triplets just above 1 ppm, each integrating for three protons. These two signals suggested the presence of two ethoxy units in the structure of TC1, resulting from chemical transformations involving the spirit ethanol. The ^{13}C NMR

384 spectrum showed 29 distinct carbon resonances out of the 31 carbon atoms presumably
385 constituting TC1. The observation of two aliphatic carbon signals resonating at 14.0 and 15.3
386 ppm was in accordance with the presence of two ethyl groups, a finding further corroborated
387 by the attribution of three signals to (oxygenated) CH_2 carbon resonances at 61.9, 63.3 and
388 65.2 ppm in the DEPT-135 spectrum. One of these CH_2 signals could be attributed to the
389 carbon atom of the primary alcohol function of the glucosidic core of TC1 (*i.e.*, C6, Table 2).
390 The ^{13}C NMR spectrum also displayed five signals resonating above 160 ppm, which could be
391 attributed to four carbonyl carbon atoms of ester functions (163.1, 168.0, 168.6 and 170.1
392 ppm), and a fifth much further downfield signal (201.9 ppm) to a ketone carbon atom.
393
394 Our hypothesis concerning the *C*-glucosidic ellagitannin nature of TC1 was then further
395 challenged by performing standard 2D NMR correlation analyses (*i.e.*, COSY, HSQC,
396 HMBC). The proton signals of the presumed open-chain glucosidic core were assigned on the
397 basis of ^{1}H-^{1}H COSY data, showing ^{3}J correlations between H1 and H2 (weak), H3 and H4
398 (strong), H4 and H5 (strong), H5 and the H6's (strong). The latter two diastereotopic protons
399 H6a and H6b resonated at 3.77 and 3.86 ppm, whose signals overlapped that of the residual
400 undeuterated water solvent. The COSY data map also revealed the presence of an ethoxy
401 group through a correlation between the methyl protons at 1.16 ppm (t, J = 7.1 Hz) and
402 methylene protons at 4.18 ppm, and that of another ethoxy group through a correlation
403 between the methyl protons at 1.09 ppm (t, J = 7.0 Hz) and two signals of similar multiplicity
404 at 3.47 and 3.59 ppm (dq, J = 9.4, 7.0 Hz). These two signals, each integrating for one proton,
405 indicated that they emanate from diastereotopic methylene protons. The same type of signals
406 was also observed in the ^{1}H spectrum of the previously described β-1-*O*-ethylvescalagin
407 (Quideau et al., 2005). Moreover, no correlation was observed with the proton signal
408 resonating at 5.40 ppm. The signals of protonated carbon atoms could then be assigned on the

409 basis of ^{1}H-^{13}C ^{1}J HSQC data, which notably indicated that C1 and C4 of the glucosidic core
410 of TC1 would have the same chemical shift at 67.8 ppm. Finally, the analysis of the ^{1}H-^{13}C
411 $^{2}J/^{3}J$ HMBC data map enabled us to determine the most likely structure of TC1. A ^{3}J
412 correlation between C1 and the methylene H1" protons at 3.47 and 3.59 ppm confirmed the
413 presence of one of the two ethoxy groups on the open-chain glucosidic core, as in the case of
414 β-1-*O*-ethylvescalagin (Quideau et al., 2005). The corollary ^{3}J correlation between H1 at 4.28
415 ppm and the methylene C1" at 65.2 ppm was also observed.
416 The other set of methylene H1'" protons resonating at 4.18 ppm were found to correlate with
417 the ester carbon atom at 170.1 ppm. Acylation of the hydroxy groups at C2, C3 and C5 of the
418 glucosidic core of TC1 by galloyl-derived units was evidenced by ^{3}J correlations between H2,
419 H3, H5 and the carbonyl CI (163.1 ppm), CII (168.0 ppm), CIII (168.6 ppm), respectively.
420 However, the more upfield shift of the carbonyl CI cast doubt on the galloyl nature of the unit
421 bearing it. Moreover, several remaining carbon signals resonating at 201.9 ppm (ketonic),
422 157.9 and 142.6 ppm (olefinic), 84.6 and 45.5 (aliphatic) remained to be assigned. In fact, it is
423 the aforementioned single proton resonance at 5.40 ppm that was the keystone of this
424 structural determination, since this H5'$_{I}$ proton, which is attached to the aliphatic C5'$_{I}$
425 resonating at 45.5 ppm (HSQC data), correlated with the ketonic C3'$_{I}$ at 201.9 ppm, the
426 olefinic C1'$_{I}$ and C2'$_{I}$ at 142.6 and 157.9 ppm, and the tertiary alcoholic C4'$_{I}$ at 84.6 ppm. In
427 addition, a ^{3}J correlation between H5'$_{I}$ and the ester carbonyl at 170.1 ppm was also observed.
428 The proximity of H5'$_{I}$ with the galloyl-derived unit II was evidenced by ^{2}J and ^{3}J correlations
429 to C-1'$_{II}$, C-2'$_{II}$, and C-3'$_{II}$. Furthermore, the olefinic C1'$_{I}$ showed a ^{3}J correlation with H1 and
430 a surprisingly strong ^{4}J correlation with H2 through the ester linkage, and the olefinic C2'$_{I}$
431 showed a ^{2}J correlation with H1.
432 All these correlation data suggested that the unit bearing the upfield (α,β-unsaturated) ester
433 carbonyl CI resonating at 163.1 ppm was a cyclopentenone moiety. The position of the ketone

function was established by observing a ^{3}J correlation between H1 and the carbonyl C3'$_{I}$ at 201.9 ppm. The cyclopentenone nature of ring I was confirmed by comparing the chemical shifts of its protons and carbons, and resonance correlations thereof, with those of the same moiety in whiskey tannin A (Fujieda et al., 2008). In fact, our TC1 is an analogue of whiskey tannin A, although it is likely not derived from castalagin but rather from its C1-epimer vescalagin. The ^{3}J coupling constant between H1 and H2 has a small value of about 1 Hz, which implies a dihedral angle close to 90° between these two protons and is hence indicative of its α-orientation at C1 (Quideau et al., 2005), whereas the same coupling constant in whiskey tannin A has a value of 3.0 Hz (Fujieda et al., 2008). Furthermore, the ROESY through-space correlation data map showed signals between H1 and H2, as well as H3, which are also consistent with an α-orientation of H1 (Figure 6, supplementary data). The configurations of the C4' and C5' centres of the cyclopentenone ring I could not be unambiguously determined, but ROESY correlations between H5'$_{I}$ and the ethoxy protons of the ester function at C4'$_{I}$ suggest that H5'$_{I}$ and this ester function are *syn*-oriented to one another. The absence of through-space correlations between H5'$_{I}$ and H1 and/or H2 cannot be used as a strong argument to confirm the β-orientation of H5'$_{I}$, especially since the correlation between H5'$_{I}$ and the β-oriented H1 was also not observed in the NOESY data of whiskey tannin A (Fujieda et al., 2008). Altogether, the interpretation of our NMR data and the comparison with literature data on analogous compounds led us to propose the structure displayed in Figure 1 and Table 2 for TC1, which we name brandy tannin A in reference to the matrix in which it was identified for the first time.

Besides the configuration at C1, the other main difference between Tanaka's whiskey tannin A and our brandy tannin A is the presence of an ethoxy group at this same C1 centre. The formation of brandy tannin A likely begins with the installation of this ethoxy group onto a

starting vescalagin in the ethanol-rich brandy solution (Figure 1). Such a formation of the resulting β-1-*O*-ethylvescalagin from vescalagin in ethanol was previously described as a relatively fast, high-yielding and diastereoselective nucleophilic substitution reaction strictly occurring with retention of configuration at C1 under standard solvolysis conditions (Quideau et al., 2005). The second step of its formation is probably the oxidative dehydrogenation of the galloyl-I group leading to the α-hydroxy-*ortho*-quinone **A**, which can then be subjected to the nucleophilic addition of ethanol at its most electrophilic carbonyl group. The resulting dienolic hemiketal **B** might then tautomerize to produce the enonic hemiketal **C**, which can then undergo a ring contraction *via* a benzilic acid-type rearrangement that forges the C–C bond between C3'$_I$ and C4'$_I$. Thus, this transformation gives rise to the formation of a cyclopentenonic ethyl ester, as previously proposed for the formation of whiskey tannins (Fujieda et al., 2008). Similar dehydrogenation-mediated contractions of ellagitannin galloyl rings into cyclopentene rings have also been previously reported (Petit et al., 2013; Tanaka et al., 1990; Wakamatsu et al., 2020). The proposed vescalagin-derived cyclopentenone is in fact the β-1-*O*-ethyl ether analogue of whiskey tannin B, hereafter referred to as brandy tannin B (Figure 1). This compound was not observed during our analyses, even though brandy tannin A certainly derives from it. In the hydroalcoholic brandy solution, the solvolytic cleavage of its hexahydroxydiphenoyl (HHDP) unit would slowly lead to the formation of brandy tannin A (TC1).

3.2.3. Gustatory properties of brandy tannin A

Brandy tannin A was then dissolved in water and in a non-oaked EDV at 2 mg/L, and the taste of each solution was characterized in comparison to the same water/EDV as a reference. Quercotriterpenoside I was used as a sweetness standard since its sensory properties have already been characterized (Marchal, Waffo-Téguo, et al., 2011). In water, brandy tannin A exhibited a slight taste of fat, no sweetness, and no bitterness. On a 0–5 scale representing

relative taste of fat and sweetness intensity assessed as a consensus between the five panelists, brandy tannin A scored 2/5 and 0/5, respectively, and QTT I was assessed as 0/5 and 3/5, respectively. Brandy tannin A was also dissolved in non-oaked EDV to study its influence on the taste balance of spirits. The control EDV was scored 0/5 for sweetness, bitterness and taste of fat, but 5/5 for the perception of burning. As a reference, EDV spiked with QTT I (2 mg/L) was described as sweeter (4/5) and less burning (2/5). Brandy tannin A also modified the taste of the EDV by significantly decreasing the perception of burning (1/5) and by significantly increasing that of sweetness (4/5).

The results suggested that brandy tannin A developed a taste of fat at 2 mg/L in water, which modulated the perception of burning of the EDV of cognac and hence improved its overall taste balance. Moreover, its taste intensity was close to that of QTT I, whose gustatory detection threshold is relatively low for non-volatile compounds (i.e. 590 μg/L in wine (Gammacurta et al., 2019), which is much lower than that of glucose, i.e., 4 g/L (Ribéreau-Gayon et al., 2017).

Koga *et al.* found a positive correlation between the antioxidant activity and the aging time of commercial whiskeys (Koga et al., 2007). In spirits, longer aging leads to a higher concentration of phenols, especially ellagic and gallic acids and lyoniresinol (Koga et al., 2007; Winstel & Marchal, 2019). These compounds play an important role in the taste of whiskey thanks to ROS (Reactive Oxygen Scavenging) and SOD (Superoxide Dismutase)-like activities (Koga et al., 2011). However, they have mostly been described as bitter (Marchal, Cretin, et al., 2015; Purwayanti, 2013), so this could not explain why spirits are known to improve during oak wood aging. Koga *et al.* also considered that there was a component of spirits which had ROS activity that offered a comfortable aftertaste rather than an unpleasant one (Koga et al., 2007). Thus, identification of brandy tannin A could provide a better understanding of the taste balance of spirits aged for a long time in barrels.

3.3. Development of an LC-HRMS method to assay brandy tannin A in spirits

From a chemical point of view, spirits are complex matrices with thousands of molecules. Consequently, specific powerful instruments are required to study their composition. Owing to its mass measurement accuracy and its wide dynamic range, LC-HRMS appeared to be a reliable technique to quantify brandy tannin A in spirits. To avoid strong matrix effects, absolute quantitation was carried out by preparing calibration solutions of brandy tannin A in a non-oaked EDV adjusted to 12% (v/v) with 0.1% of formic acid. In this study, LOD and LOQ were established at 1 µg/L and 2 µg/L, respectively. A calibration curve was obtained with a good correlation coefficient (R^2 of 0.999) for a range from 2 µg/L to 10 mg/L, this validating the linearity of the method. Moreover, all the samples had concentrations that were in the working range, which confirmed the relevance of the latter. The recovery of back-calculated concentrations was higher than 90% at each method calibration level, thus establishing the accuracy of the method. Intraday repeatability for each concentration was lower than 4.2%. Interday repeatability was not as good at low concentrations (up to 16% at 10 µg/L) but efficient at 10 mg/L (<5%). To overcome this issue, all calibration solutions were injected for each quantitative analysis of an unknown sample. Two spirits spiked with stock solutions were also injected. Recovery ratios ranged from 94 to 105%, which is in accordance with common specifications (Guidance for Industry, 2018). Consequently, these results established the repeatability and the trueness of the method applied to spirits. Analysis of the above samples revealed small variations in retention time (<0.02 min) and a mass deviation lower than 0.9 ppm at various concentrations, guaranteeing the specificity of the method. All these results validated the LC-HRMS method to quantitate brandy tannin A in spirits (Table 3).

3.4. Quantification of brandy tannin A in spirits

3.4.1. Evolution of brandy tannin A over 8 years

Brandy tannin A was quantitated in samples of EDV of cognac of nine different vintages from the same distillery (Table S7, Supplementary data). The samples were not commercial cognac but EDV which have been aged in barrels since 2010. A sample was collected each year from the same barrel from 2010 to 2018, so the 2011 sample corresponds to one year of aging in barrels, the one of 2012 to 2 years and so on. Brandy tannin A was detected and quantitated in all spirits at a concentration of 100 µg/L for the sample aged for 1 year in barrels. This result suggested that it was formed quite quickly after the beginning of aging. The contents of brandy tannin A were higher in old vintages, reaching a concentration of 2 mg/L for the oldest sample which had been aged in barrels for 8 years (Figure 2, A). Long barrel aging appeared to promote the formation of brandy tannin A. Moreover, its reaction rate appeared to be proportional to its concentration and could be compared to first-order kinetics.

3.4.2. Content of brandy tannin A in various vintages of same spirits

Brandy tannin A was also assayed in the samples of EDV of cognac previously used for untargeted metabolomic analysis (Table S8, Supplementary data). The concentrations in Figure 2 correspond to the mean values of the five replicates for the spirits from 2015 to 1990, and of four replicates for the last two vintages (Figure 2, B). The measured values ranged from 0.4 mg/L (2015) to 4.2 mg/L (1995). For each vintage, the coefficient of variation between the replicates was relatively low (from 12.7% to 36.6%), so the heterogeneity between barrels was not too high, except for the 2005 vintage (47.2%). The evolution of concentrations for the vintages from 2015 to 2005 was consistent with that of the first series of spirits. However, brandy tannin A concentrations seemed to follow a bell-shaped curve; low in the 2015 sample (0.4 mg/L), maximal in the 1995 sample (4.2 mg/L) and lower in older vintages (e.g. 0.7 mg/L for the 1970 vintage). These results were consistent with its relative quantitation (Figure S4, Supplementary data) obtained by the untargeted metabolomic approach, in which the same trend was observed. Even if this was not a strict kinetic study as

559 in the first series of EDV of cognac, this suggested its degradation with barrel aging.
560 However, this hypothesis needs to be studied more deeply, since the results could also have
561 been due to modifications of aging practices in the distillery or to changes in barrel supplies.

562 Moreover, six of the ten vintages had concentrations greater than 2 mg/L. Sensory
563 studies showed significant taste modifications at this concentration, thus demonstrating its
564 contribution to the taste balance of these spirits. Spirits are known to improve during oak
565 wood aging and brandy tannin A might play a key role in modulating their taste balance.

566 *3.4.3. Content of brandy tannin A in various commercial spirits*

567 Thirty-six commercial spirits were also analysed to measure the concentration of brandy
568 tannin A (Table S9, Supplementary data). It was detected in almost all cognacs at
569 concentrations ranging from 0.03 to 7.7 mg/L but also in two brandies, two whiskeys and one
570 rum, in smaller quantities (from 0.01 to 0.4 mg/L) (Figure 3). In addition, two Japanese
571 whiskeys (W-6 and W-7, Figure 3) were analysed since the whiskey tannins A and B have
572 already been purified from this kind of spirits (Fujieda et al., 2008). Results showed very low
573 levels of brandy tannin A (< 13 µg/L) in these spirits. The higher brandy tannin A
574 concentration in the C-7 sample could be due to the significant addition of "boisé" (aqueous
575 extract of oak wood chips) to this spirit, which is permitted by law for some brandies. The
576 differences in concentration between the other spirits could be due to the botanical origin of
577 the wood used for aging. Bourbons are aged in American oak barrels, while cognacs and
578 brandies are generally aged in French sessile or pedunculate oak barrels. In addition, this
579 result did not seem surprising since American oaks are known to have much lower
580 concentrations of ellagitannins than pedunculate oak (Chatonnet & Dubourdieu, 1988).
581 Additional studies will be necessary to validate this hypothesis. The influence of cooperage
582 parameters such as the botanical origin of oak wood on brandy tannin A concentrations could

be studied. A better control of this parameter could improve the monitoring of oak wood aging and its sensory effect.

4. Conclusion

This study focused on discovering new taste-active compounds formed during spirits aging in barrels. For this purpose, an untargeted metabolomic profiling by HRMS in negative mode was performed on EDV of cognac from several vintages. After statistical analysis, TC1 was found to be significantly more abundant in spirits than in oak wood, which could suggest its neoformation. After the development of a fractionation protocol, brandy tannin A (*i.e.*, TC1) was identified and purified from a blend of old EDVs of cognac. To our knowledge, its identification, its presence in spirits, mostly in cognacs, and its sensory properties have never been described until now. Moreover, its impact on the spirits taste balance was perceived more strongly by decreasing the burning perception. By determining its gustatory detection threshold, it might be possible to establish its influence during aging on the taste balance of old spirits. It would also be interesting to measure its ROS activity to attest to its comfortable aftertaste. Its concentrations in several EDV of cognac seemed to follow a bell-shaped curve, suggesting the competition of two phenomena: its formation from a native oak precursor and its degradation. In both cases, it will be necessary to clarify the chemical species involved, the reaction mechanisms and the factors that could influence their evolution. The present findings illustrate the efficiency of our novel method, which allowed the purification of a new ellagitannin from highly complex mixtures. In future work, such a strategy could be used to reveal new sensory-active products in natural matrices.

Acknowledgements

Delphine Winstel grant is funded by Remy-Martin and Seguin-Moreau. The authors are also grateful to J.-C. Mathurin and L. Urruty for providing samples. We thank Dr. Ray Cooke for proofreading the manuscript.

Competing interest statement

The authors declare no competing financial interest.

Author contributions

Delphine Winstel: Conceptualization, Methodology, Investigation, Validation, Writing – Original Draft

Yoan Capello: Conceptualization, Validation, Writing – Original Draft

Stéphane Quideau: Conceptualization, Validation, Writing – Review and editing, Visualization

Axel Marchal: Conceptualization, Validation, Writing – Review and editing, Supervision, Funding acquisition

References

Auzanneau, C., Montaudon, D., Jacquet, R., Puyo, S., Pouységu, L., Deffieux, D., Elkaoukabi-Chaibi, A., De Giorgi, F., Ichas, F., Quideau, S., & Pourquier, P. (2012). The Polyphenolic Ellagitannin Vescalagin Acts As a Preferential Catalytic Inhibitor of the α Isoform of Human DNA Topoisomerase II. *Molecular Pharmacology*, *82*(1), 134–141. https://doi.org/10.1124/mol.111.077537

Bowers, J. J., Gunawardena, H. P., Cornu, A., Narvekar, A. S., Richieu, A., Deffieux, D., Quideau, S., & Tharayil, N. (2018). Rapid Screening of Ellagitannins in Natural Sources via Targeted Reporter Ion Triggered Tandem Mass Spectrometry. *Scientific Reports*, *8*(1), 1–10. https://doi.org/10.1038/s41598-018-27708-3

Cardullo, N., Muccilli, V., Pulvirenti, L., Cornu, A., Pouységu, L., Deffieux, D., Quideau, S., & Tringali, C. (2020). C-glucosidic ellagitannins and galloylated glucoses as potential functional food ingredients with anti-diabetic properties: A study of α-glucosidase and α-amylase inhibition. *Food Chemistry*, *313*, 126099. https://doi.org/10.1016/j.foodchem.2019.126099

Chassaing, S., Lefeuvre, D., Jacquet, R., Jourdes, M., Ducasse, L., Galland, S., Grelard, A., Saucier, C., Teissedre, P.-L., Dangles, O., & Quideau, S. (2010). Physicochemical Studies of New Anthocyano-Ellagitannin Hybrid Pigments: About the Origin of the Influence of Oak C-Glycosidic Ellagitannins on Wine Color. *European Journal of Organic Chemistry*, *2010*(1), 55–63. https://doi.org/10.1002/ejoc.200901133

Chatonnet, P., & Dubourdieu, D. (1988). Comparative Study of the Characteristics of American White Oak (Quercus alba) and European Oak (Quercus petraea and Q. robur) for Production of Barrels Used in Barrel Aging of Wines | American Journal of Enology and Viticulture. *Am. J. Enol. Vitic.*, *49*(1), 79–85.

Chira, K., Zeng, L., Le Floch, A., Péchamat, L., Jourdes, M., & Teissedre, P.-L. (2015). Compositional and sensory characterization of grape proanthocyanidins and oak wood ellagitannin. *Tetrahedron*, *71*(20), 2999–3006. https://doi.org/10.1016/j.tet.2015.02.018

Cretin, B. N., Waffo-Teguo, P., Dubourdieu, D., & Marchal, A. (2019). Taste-guided isolation of sweet-tasting compounds from grape seeds, structural elucidation and identification in wines. *Food Chemistry*, *272*, 388–395. https://doi.org/10.1016/j.foodchem.2018.08.070

De Paepe, D., Servaes, K., Noten, B., Diels, L., De Loose, M., Van Droogenbroeck, B., & Voorspoels, S. (2013). An improved mass spectrometric method for identification and quantification of phenolic compounds in apple fruits. *Food Chemistry*, *136*(2), 368–375. https://doi.org/10.1016/j.foodchem.2012.08.062

Engström, M. T., Pälijärvi, M., & Salminen, J.-P. (2015). Rapid Fingerprint Analysis of Plant Extracts for Ellagitannins, Gallic Acid, and Quinic Acid Derivatives and Quercetin-, Kaempferol- and Myricetin-Based Flavonol Glycosides by UPLC-QqQ-MS/MS. *Journal of Agricultural and Food Chemistry*, *63*(16), 4068–4079. https://doi.org/10.1021/acs.jafc.5b00595

Fayad, S., Le Scanff, M., Waffo-Teguo, P., & Marchal, A. (2021). Understanding sweetness of dry wines: First evidence of astilbin isomers in red wines and quantitation in a one-century range of vintages. *Food Chemistry*, *352*, 129293. https://doi.org/10.1016/j.foodchem.2021.129293

Frank, O., Zehentbauer, G., & Hofmann, T. (2006). Bioresponse-guided decomposition of roast coffee beverage and identification of key bitter taste compounds. *European Food Research and Technology*, *222*(5), 492. https://doi.org/10.1007/s00217-005-0143-6

669 Fujieda, M., Tanaka, T., Suwa, Y., Koshimizu, S., & Kouno, I. (2008). Isolation and Structure
670 of Whiskey Polyphenols Produced by Oxidation of Oak Wood Ellagitannins. *Journal*
671 *of Agricultural and Food Chemistry*, *56*(16), 7305–7310.
672 https://doi.org/10.1021/jf8012713
673 Gadrat, M., Lavergne, J., Emo, C., Teissedre, P.-L., & Chira, K. (2020). Validation of a mass
674 spectrometry method to identify and quantify ellagitannins in oak wood and cognac
675 during aging in oak barrels. *Food Chemistry*, 128223.
676 https://doi.org/10.1016/j.foodchem.2020.128223
677 Gammacurta, M., Waffo-Teguo, P., Winstel, D., Cretin, B. N., Sindt, L., Dubourdieu, D., &
678 Marchal, A. (2019). Triterpenoids from Quercus petraea: Identification in Wines and
679 Spirits and Sensory Assessment. *Journal of Natural Products*, *82*(2), 265–275.
680 https://doi.org/10.1021/acs.jnatprod.8b00682
681 Georgess, D., Spuul, P., Le Clainche, C., Le Nihouannen, D., Fremaux, I., Dakhli, T.,
682 Delannoy López, D. M., Deffieux, D., Jurdic, P., Quideau, S., & Génot, E. (2018).
683 Anti-osteoclastic effects of C-glucosidic ellagitannins mediated by actin perturbation.
684 *European Journal of Cell Biology*, *97*(8), 533–545.
685 https://doi.org/10.1016/j.ejcb.2018.09.003
686 Glabasnia, A., & Hofmann, T. (2006). Sensory-Directed Identification of Taste-Active
687 Ellagitannins in American (*Quercus alba* L.) and European Oak Wood (*Quercus*
688 *robur* L.) and Quantitative Analysis in Bourbon Whiskey and Oak-Matured Red
689 Wines. *Journal of Agricultural and Food Chemistry*, *54*(9), 3380–3390.
690 https://doi.org/10.1021/jf052617b
691 Guidance for Industry. (2018). Bioanalytical Method Validation. *U.S. Department of Health*
692 *and Human Services, Food and Drug Administration, Center for Drug Evaluation and*
693 *Research (CDER), Center for Veterinary Medicine (CVM).*

ISO 3591:1977. (1977). Analyse sensorielle—Appareillage—Verre à dégustation pour l'analyse sensorielle des vins. In *Analyse sensorielle: Recueil, normes, agroalimentaire*. https://www.iso.org/fr/standard/9002.html

ISO 8589:2010. (2010). Analyse sensorielle—Directives générales pour la conception de locaux destinés à l'analyse. In *Analyse sensorielle: Recueil, normes, agroalimentaire*. AFNOR. https://www.boutique.afnor.org/norme/nf-en-iso-8589/analyse-sensorielle-directives-generales-pour-la-conception-de-locaux-destines-a-l-analyse/article/784220/fa165403

Jourdes, M., Michel, J., Saucier, C., Quideau, S., & Teissedre, P.-L. (2011). Identification, amounts, and kinetics of extraction of C-glucosidic ellagitannins during wine aging in oak barrels or in stainless steel tanks with oak chips. *Analytical and Bioanalytical Chemistry*, *401*(5), 1531–1539. https://doi.org/10.1007/s00216-011-4949-8

Kinghorn, A. D. (1987). Biologically Active Compounds from Plants with Reputed Medicinal and Sweetening Properties. *Journal of Natural Products*, *50*(6), 1009–1024. https://doi.org/10.1021/np50054a002

Koga, K., Tachihara, S., Shirasaka, N., Yamada, Y., & Koshimizu, S.-I. (2011). Profile of non-volatiles in whisky with regard to superoxide dismutase activity. *Journal of Bioscience and Bioengineering*, *112*(2), 154–158. https://doi.org/10.1016/j.jbiosc.2011.04.002

Koga, K., Taguchi, A., Koshimizu, S., Suwa, Y., Yamada, Y., Shirasaka, N., & Yoshizumi, H. (2007). Reactive Oxygen Scavenging Activity of Matured Whiskey and Its Active Polyphenols. *Journal of Food Science*, *72*(3), S212–S217. https://doi.org/10.1111/j.1750-3841.2007.00311.x

Marchal, A., Cretin, B. N., Sindt, L., Waffo-Téguo, P., & Dubourdieu, D. (2015). Contribution of oak lignans to wine taste: Chemical identification, sensory

719 characterization and quantification. *Tetrahedron*, *71*(20), 3148–3156.
720 https://doi.org/10.1016/j.tet.2014.07.090
721 Marchal, A., Génin, E., Waffo-Téguo, P., Bibès, A., Da Costa, G., Mérillon, J.-M., &
722 Dubourdieu, D. (2015). Development of an analytical methodology using Fourier
723 transform mass spectrometry to discover new structural analogs of wine natural
724 sweeteners. *Analytica Chimica Acta*, *853*, 425–434.
725 https://doi.org/10.1016/j.aca.2014.10.039
726 Marchal, A., Marullo, P., Moine, V., & Dubourdieu, D. (2011). Influence of Yeast
727 Macromolecules on Sweetness in Dry Wines: Role of the Saccharomyces cerevisiae
728 Protein Hsp12. *Journal of Agricultural and Food Chemistry*, *59*(5), 2004–2010.
729 https://doi.org/10.1021/jf103710x
730 Marchal, A., Pons, A., Lavigne, V., & Dubourdieu, D. (2013). Contribution of oak wood
731 ageing to the sweet perception of dry wines: Effect of oak ageing on wine sweetness.
732 *Australian Journal of Grape and Wine Research*, *19*(1), 11–19.
733 https://doi.org/10.1111/ajgw.12013
734 Marchal, A., Waffo-Téguo, P., Génin, E., Mérillon, J.-M., & Dubourdieu, D. (2011).
735 Identification of New Natural Sweet Compounds in Wine Using Centrifugal Partition
736 Chromatography–Gustatometry and Fourier Transform Mass Spectrometry. *Analytical*
737 *Chemistry*, *83*(24), 9629–9637. https://doi.org/10.1021/ac202499a
738 Petit, E., Lefeuvre, D., Jacquet, R., Pouységu, L., Deffieux, D., & Quideau, S. (2013).
739 Remarkable Biomimetic Chemoselective Aerobic Oxidation of Flavano-Ellagitannins
740 Found in Oak-Aged Wine. *Angewandte Chemie International Edition*, *52*(44), 11530–
741 11533. https://doi.org/10.1002/anie.201305839
742 Pluskal, T., Castillo, S., Villar-Briones, A., & Orešič, M. (2010). MZmine 2: Modular
743 framework for processing, visualizing, and analyzing mass spectrometry-based

molecular profile data. *BMC Bioinformatics*, *11*(1), 395. https://doi.org/10.1186/1471-2105-11-395

Puech, J. L., Rabier, P., Bories-Azeau, J., Sarni, F., & Moutounet, M. (1990). Determination of ellagitannins in extracts of oak wood and in distilled beverages matured in oak barrels. *Journal - Association of Official Analytical Chemists*, *73*(4), 498–501.

Purwayanti, S. (2013). Taste Compounds from Crude Extract of Bekkai lan (Albertisia papuana Becc.). *Journal of Food and Nutrition Sciences*, *1*(4), 33. https://doi.org/10.11648/j.jfns.20130104.11

Quideau, S., Jourdes, M., Lefeuvre, D., Montaudon, D., Saucier, C., Glories, Y., Pardon, P., & Pourquier, P. (2005). The Chemistry of Wine PolyphenolicC-Glycosidic Ellagitannins Targeting Human Topoisomerase II. *Chemistry - A European Journal*, *11*(22), 6503–6513. https://doi.org/10.1002/chem.200500428

Ribéreau-Gayon, P., Glories, Y., Maujean, A., & Dubourdieu, D. (2017). *Traité d'oenologie—Tome 2—7e éd. - Chimie du vin. Stabilisation et traitements*. Dunod.

Roullier-Gall, C., Signoret, J., Hemmler, D., Witting, M. A., Kanawati, B., Schäfer, B., Gougeon, R. D., & Schmitt-Kopplin, P. (2018). Usage of FT-ICR-MS Metabolomics for Characterizing the Chemical Signatures of Barrel-Aged Whisky. *Frontiers in Chemistry*, *6*. https://doi.org/10.3389/fchem.2018.00029

Saucier, C., Jourdes, M., Glories, Y., & Quideau, S. (2006). Extraction, Detection, and Quantification of Flavano-Ellagitannins and Ethylvescalagin in a Bordeaux Red Wine Aged in Oak Barrels. *Journal of Agricultural and Food Chemistry*, *54*(19), 7349–7354. https://doi.org/10.1021/jf061724i

Tanaka, T., Nonaka, G., & Nishioka, I. (1990). Tannins and Related Compounds. C.: Reaction of Dehydrohexahydroxydiphenic Acid Esters with Bases, and Its Application

768 to the Structure Determination of Pomegranate Tannins, Granatins A and B. *Chemical*
769 *& Pharmaceutical Bulletin*, *38*(9), 2424–2428. https://doi.org/10.1248/cpb.38.2424
770 Viriot, C., Scalbert, A., Lapierre, C., & Moutounet, M. (1993). Ellagitannins and lignins in
771 aging of spirits in oak barrels. *Journal of Agricultural and Food Chemistry*, *41*(11),
772 1872–1879.
773 Wakamatsu, H., Matsuo, Y., Omar, M., Saito, Y., Nishida, K., & Tanaka, T. (2020).
774 Oxidation of the Oak Ellagitannin, Vescalagin. *Journal of Natural Products*, *83*(2),
775 413–421. https://doi.org/10.1021/acs.jnatprod.9b00917
776 Winstel, D., Bahammou, D., Albertin, W., Waffo-Téguo, P., & Marchal, A. (2021).
777 Untargeted LC–HRMS profiling followed by targeted fractionation to discover new
778 taste-active compounds in spirits. *Food Chemistry*, *359*, 129825.
779 https://doi.org/10.1016/j.foodchem.2021.129825
780 Winstel, D., Gautier, E., & Marchal, A. (2020). Role of Oak Coumarins in the Taste of Wines
781 and Spirits: Identification, Quantitation, and Sensory Contribution through Perceptive
782 Interactions. *Journal of Agricultural and Food Chemistry*, acs.jafc.0c02619.
783 https://doi.org/10.1021/acs.jafc.0c02619
784 Winstel, D., & Marchal, A. (2019). Lignans in Spirits: Chemical Diversity, Quantification,
785 and Sensory Impact of (±)-Lyoniresinol. *Molecules*, *24*(1), 117.
786 https://doi.org/10.3390/molecules24010117
787

Abbreviations

EDV : “eau-de-vie”

PCA: Principal component analysis

TC1: Targeted Compound 1

LOD: limit of detection

LOQ: limit of quantitation

Appendix A. Supplementary data

Table S1: Features of "eaux-de-vie" of cognac used for untargeted LC-HRMS approach.

Figure S2: Representation of different groups of compounds according to their evolution in 48 "eaux-de-vie" of cognac.

Figure S3: Negative LC-ESI-FTMS XIC of an oaked "eau-de-vie" of cognac (A, on the left), an oak wood extract (B, on the right) corresponding to a negative ion at *m/z* 703.1143.

Figure S4: Evolution of TC1 in the "eau-de-vie" of cognac from 2015 to 1970. *Error bars* represent standard deviation of different replicates.

Figure S5: HRMS spectrum of TC1 (with fragmentation 35 eV).

Figure S6: ^{1}H, ^{13}C, DEPT-135, COSY, HSQC, HMBC, ROESY NMR spectra and correlation data map of brandy tannin A (TC1) in acetone-D_6/D_2O (9:1, v/v) at 400 MHz and 600 MHz.

Table S7: Individual concentrations of brandy tannin A in 9 vintages of same spirit. All concentrations expressed in (mg/L).

Table S8: Individual concentrations of brandy tannin A in 10 vintages of same spirit. All concentrations expressed in (mg/L).

Table S9: Individual concentrations of brandy tannin A in 36 commercial spirits. All concentrations expressed in (mg/L).

821 **FIGURES AND TABLES**

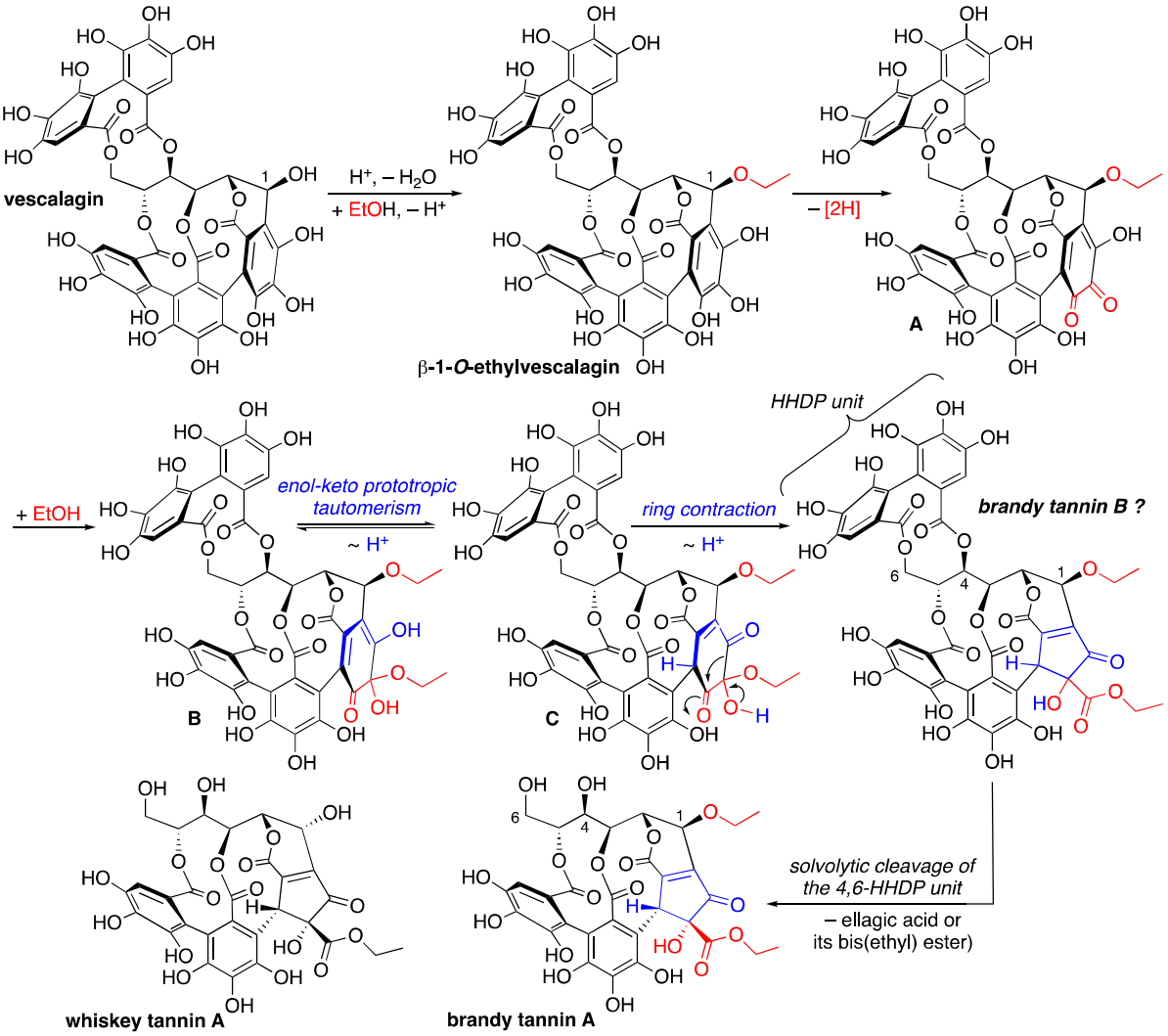

822

823 **Figure 1.** Mechanistic depiction of formation of brandy tannin A from vescalagin.

824

825

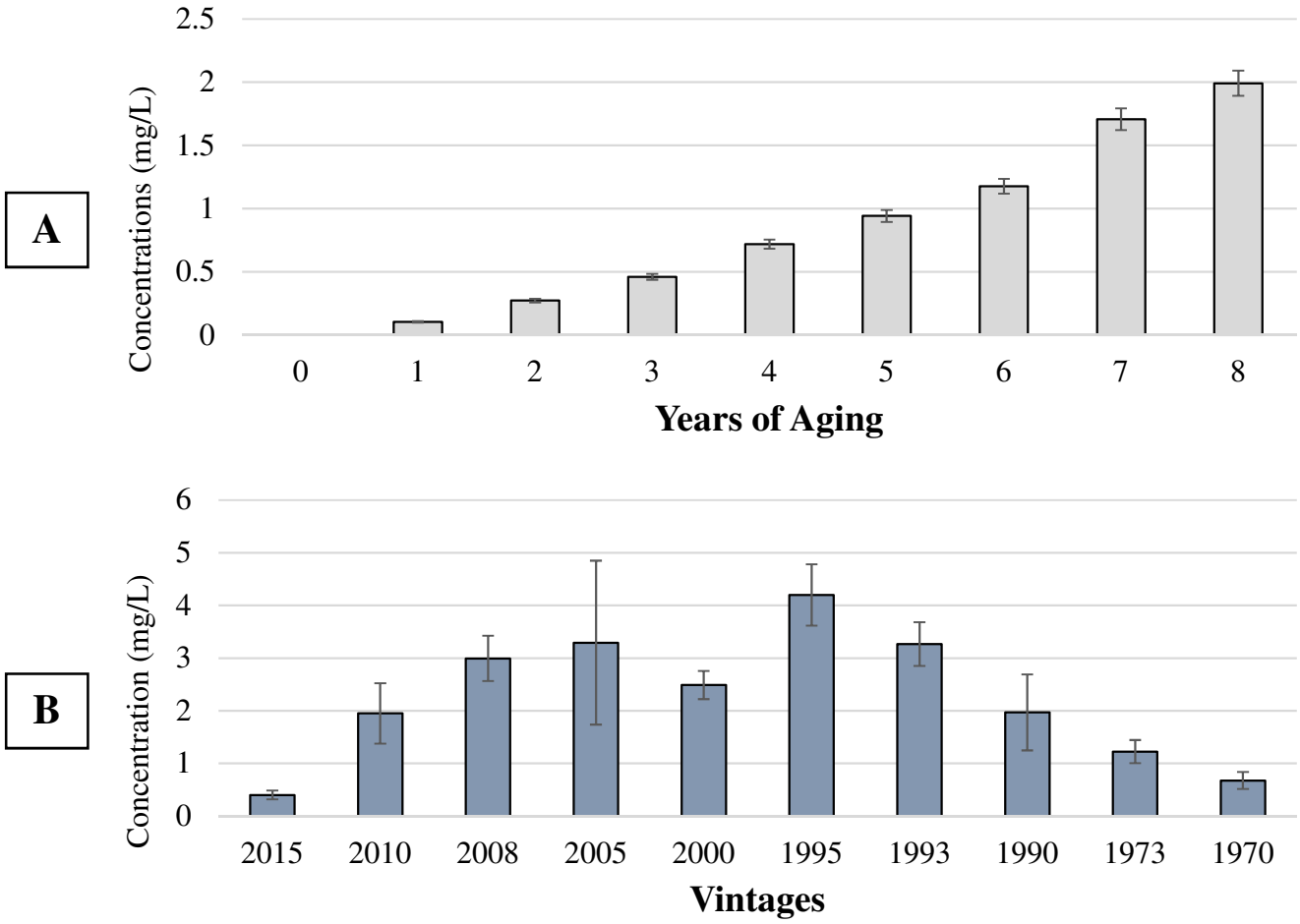

826 **Figure 2**: Concentrations of brandy tannin A over 8 years of aging in barrels (**A**) and in 10
827 vintages of "eau-de-vie" of cognac from same distillery (**B**).

828

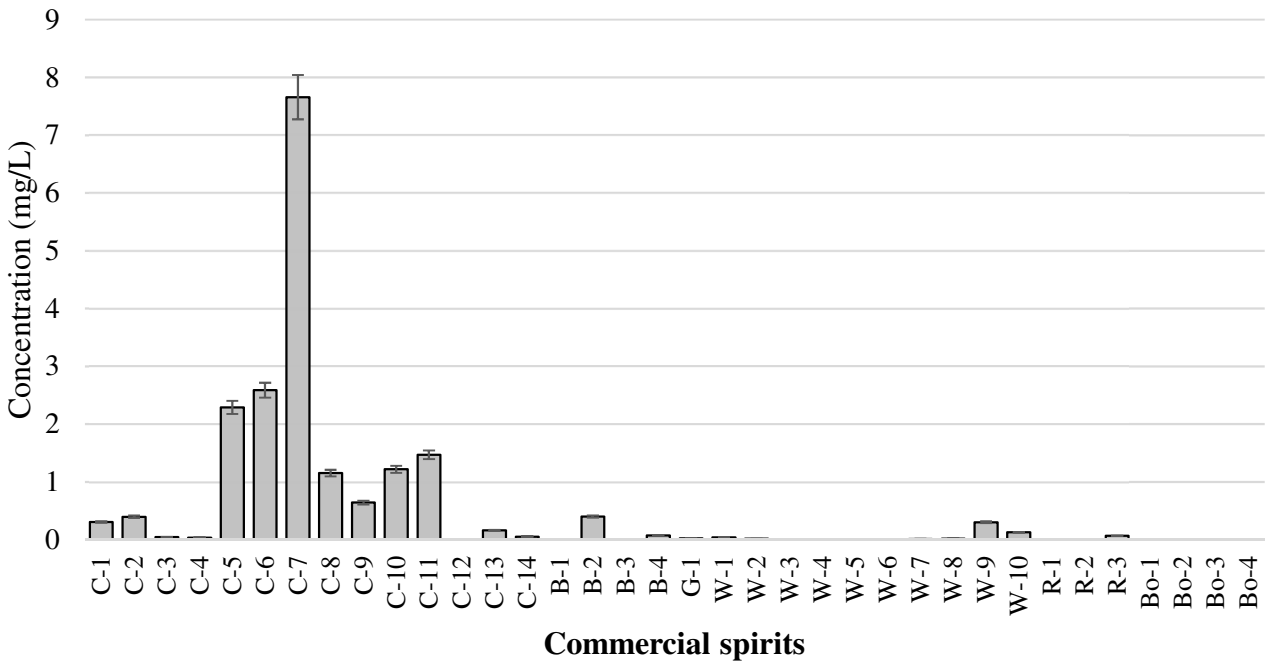

829

830 **Figure 3**: Concentrations of brandy tannin A in 36 commercial spirits (C: Cognac; B: Brandy;
831 G: Gin; W: Whisky; R: Rum; Bo: Bourbon).

832

833 **Table 1.** Ionization and spectrometric conditions for HRMS analyses.

Ionization mode	**Negative**			
Mass Spectrometer	**Q-Exactive Plus**		**Exactive**	
Use	LC-MS^n Metabolomic approach		LC-HRMS Screening	LC-HRMS Quantitation
Mass scan	Full MS	dd-MS^2	Full MS	Full MS
Sheath gas flow [a]	48		70	60
Auxiliary gas flow [a]	11		15	15
Spare gas flow [a]	2		0	0
HESI probe temperature	300 °C		320 °C	350 °C
Capillary temperature	300 °C		350 °C	300 °C
Electrospray voltage	- 3.3 kV		- 3.5 kV	- 3.5 kV
S-lens RF level [b]	55		-	-
Capillary voltage	-		- 25 V	- 95 V
Tube lens voltage offset	-		- 120 V	- 160 V
Skimmer voltage	-		- 20 V	- 18 V
Mass range (in Th)	100 - 1500	200 - 2000	200 - 1000	200 - 1000
Resolution [c]	35,000	17,500	25,000	10,000
AGC value [d]	10^6 ions	10^5 ions	10^6 ions	3.10^6 ions
Maximum injection time	60 ms	50 ms	-	-
Fragmentation	-	28 eV	-	-

834 [a] Sheath gas, auxiliary gas and spare gas flows (all nitrogen) are expressed in arbitrary units

835 [b] S-lens RF level are expressed in arbitrary units

836 [c] Resolution $m/\Delta m$, fwhm at m/z 200 Th

837 [d] Automatic Gain Control

838

839 **Table 2.** ^{1}H and ^{13}C NMR signal assignments of brandy tannin A (TC1).

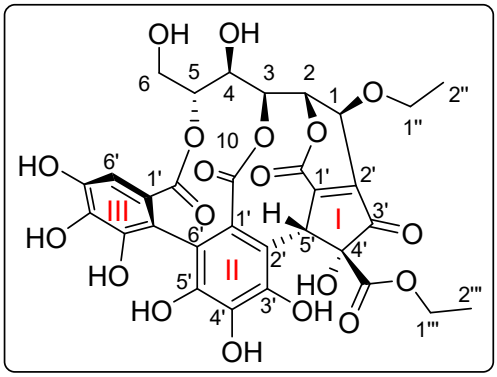

840
841

Position	δ_{H} (J = Hz)	δ_{C}	HSQC	HMBC / COSY
Glucose				
1	4.28 (*d*, 1.1)	67.8	C-1	H-2, H-3, C-1", C-2, C-3, C-1'$_{I}$, C-2'$_{I}$, C-3'$_{I}$
2	5.48 (*d*, 1.0)	80.3	C-2	H-1, H-3, C-1, C-1'$_{I}$, C$_{I}$=O
3	5.32 (*d*, 6.7)	72.7	C-3	H-2, H-4, C-4, C$_{II}$=O
4	4.40 (*dd*, 9.3, 6.7)	67.8	C-4	H-3, H-5, C-6, C-3, C-5
5	4.90 (*ddd*, 9.3, 4.3, 2.8)	74.8	C-5	H-3, H-4, H-6, C-4, C$_{III}$=O
6	3.77 (*m*) 3.86 (*m*)	61.9	C-6	H-5, C-4
Cyclopentenone				
1'$_{I}$		142.6		H-1, H-2, H-5'$_{I}$,
2'$_{I}$		157.9		H-1, H-5'$_{I}$
3'$_{I}$		201.9		H-1, H-5'$_{I}$
4'$_{I}$		84.6		H-5'$_{I}$
5'$_{I}$	5.40 (*s*)	45.5	C-5'$_{I}$	C-1'$_{I}$, C-2'$_{I}$, C-3'$_{I}$, C-4'$_{I}$, C-1'$_{II}$, C-2'$_{II}$, C-3'$_{II}$, C=O$_{Ester}$
Aromatics				
1'$_{II}$		125.0		H-5'$_{I}$
1'$_{III}$		125.4		
2'$_{II}$		111.0		H-5'$_{I}$
2'$_{III}$		113.5		H-6'$_{III}$
3'$_{II}$		146.0		H-5'$_{I}$
3'$_{III}$		144.5		H-6'$_{III}$
4'$_{II}$		135.4		
4'$_{III}$		136.6		H-6'$_{III}$
5'$_{II}$		144.5		H-5'$_{I}$
5'$_{III}$		145.5		H-6'$_{III}$
6'$_{II}$		114.7		
6'$_{III}$	6.69 (*s*)	108.1	C-6'$_{III}$	C-2'$_{III}$, C-3'$_{III}$, C-

				4'$_{III}$, C$_{III}$=O, C-5'$_{III}$
Carbonyls				
C=O$_{ester}$		170.1		H-1", H-5'$_{I}$
C$_{I}$=O		163.1		H-2
C$_{II}$=O		168.0		H-3
C$_{III}$=O		168.6		H-5, H-6'$_{III}$
Ethyl ether				
1"	3.47 (*dq*, 9.3, 7.0) 3.59 (*dq*, 9.4, 7.0)	65.2	C-1"	H-2", C-1, C-2"
2"	1.09 (*t*, 7.0)	15.3	C-2"	H-1", C-1"
Ethyl ester				
1'"	4.18 (m)	63.3	C-1'"	H-2'", C-2'", C=O$_{ester}$
2'"	1.16 (*t*, 7.1)	14.0	C-2'"	H-1'", C-1'"

842

843

844 **Table 3**: Validation parameters for HRMS quantitation of brandy tannin A in spirits.
845

Parameters		**Matrix - Spirits**		
Sensitivity		**LOD (µg/L)**	**LOQ (µg/L)**	
		1	2	
Linearity and accuracy		**Working range**	**R^2**	
		2 µg/L - 10 mg/L	0.999	
Specificity		**t_R variation**	**Mass accuracy**	
		0.02 min	0.9 ppm	
Repeatability and trueness		**Intraday repeatability**		
		10 µg/L	*200 µg/L*	*10 mg/L*
		4.2%	2.7%	2.4%
		Interday repeatability		
		10 µg/L	*10 mg/L*	
		16.3%	4.2%	
		Recovery		
		20 µg/L	*200 µg/L*	*10 mg/L*
	EDV-1	102%	102%	94%
	EDV-2	105%	100%	94%

846

847

Graphical abstract